Received: 10 March 2020 | Revised: 14 July 2020

DOI: 10.1111/sapm.12334

ORIGINAL ARTICLE

STUDIES IN APPLIED MATHEMATICS WILEY

Multiscale expansions avector solitons of a two-dimensional nonlocal nonlinear Schrödinger system

Georgios N. Koutsokostas[1] | **Theodoros P. Horikis**[2] | **Dimitrios J. Frantzeskakis**[1] | **Barbara Prinari**[3] | **Gino Biondini**[3]

[1] Department of Physics, National and Kapodistrian University of Athens, Athens, Greece

[2] Department of Mathematics, University of Ioannina, Ioannina, Greece

[3] Department of Mathematics, State University of New York at Buffalo, Buffalo, New York

Correspondence
Theodoros P. Horikis, Department of Mathematics, University of Ioannina, Ioannina 45110, Greece.
Email: horikis@uoi.gr

Abstract

One- and two-dimensional solitons of a multicomponent nonlocal nonlinear Schrödinger (NLS) system are constructed. The model finds applications in nonlinear optics, where it may describe the interaction of optical beams of different frequencies. We asymptotically reduce the model, via multiscale analysis, to completely integrable ones in both Cartesian and cylindrical geometries; we thus derive a Kadomtsev-Petviashvili equation and its cylindrical counterpart, Johnson's equation. This way, we derive approximate soliton solutions of the nonlocal NLS system, which have the form of: (a) dark or antidark soliton stripes and (b) dark lumps in the Cartesian geometry, as well as (c) ring dark or antidark solitons in the cylindrical geometry. The type of the soliton, namely dark or antidark, is determined by the degree of nonlocality: dark (antidark) soliton states are formed for weaker (stronger) nonlocality. We perform numerical simulations and show that the derived soliton solutions do exist and propagate undistorted in the original nonlocal NLS system.

KEYWORDS

dark and antidark solitons, KP equations, multiple scales analysis, nonlocal coupled NLS

1 INTRODUCTION

Many problems in nonlinear waves can be greatly simplified by using asymptotic multiscale expansion methods that lead to nonlinear evolution equations that are much simpler than a specific problem at hand.[1] The use of such asymptotic methods has led to a number of interesting findings. For instance, it has been shown that models that are completely integrable by the Inverse Scattering Transform (IST)[2] can be reduced to other integrable models.[3] A characteristic example is the asymptotic reduction of the defocusing nonlinear Schrödinger (NLS) equation to the Korteweg-de Vries (KdV) equation, which led to the discovery of dark solitons, and particularly to the description of shallow NLS dark solitons in terms of KdV solitons.[4] Perhaps even more interestingly, relevant connections have also been proposed for nonintegrable models. This is particularly important, because exact solutions of the reduced equations can be used for the derivation of approximate solutions of the original nonintegrable models. Relevant studies continue up till now (see, e.g., Ref. 5), and have provided insights in studies of solitons in various physical contexts, such as nonlinear optics[6] and Bose-Einstein condensation.[7,8]

Multiscale expansion methods become particularly relevant and helpful in cases where the original system does not possess solutions in explicit form. A particularly interesting example is a class of NLS equations with a spatially nonlocal nonlinearity. Such nonlocal NLS models arise, for example, in the description of optical beam dynamics and solitons in plasmas,[9] atomic vapors,[10] lead glasses with a thermal nonlinearity,[11] as well as in media with long-range interactions, such as nematic liquid crystals[12] and dipolar Bose gases.[13] Note that a variant of a nonlocal NLS model, namely the Schrödinger-Poisson equation, appears also in cosmology, where it may describe the dynamics of coherent dark matter made up of ultralight axions (see, e.g., Ref. 14 and references therein).

Importantly, nonlocality can dramatically affect the soliton properties. For instance, in higher dimensional settings with a nonlocal focusing nonlinear response, collapse can be arrested[15,16] and stable solitons can be formed; see relevant experimental[10,11] and theoretical[17] results, as well as the reviews[16,18] and references therein. On the other hand, if nonlocal nonlinearity is of the defocusing type, dark solitons do exist,[19–22] and may even feature an attractive interaction[19] (note that, in the case of a local defocusing nonlinearity, dark solitons always repel each other[6–8]). Furthermore, in higher dimensional settings, dark solitons that are typically prone to the transverse (or "snaking") instability[8,23–25] can be stabilized due to nonlocality.[26]

Motivated by the above, here we study a multicomponent nonlocal NLS system in $(2+1)$-dimensions, which may describe the interaction of optical beams of different frequencies in the above-mentioned nonlocal media. We present asymptotic reductions of the model to the Kadomtsev-Petviashvili (KP) equation in the Cartesian setting (see, e.g., Ref. 27), as well as to its cylindrical version, known as the Johnson's equation;[28] such KP models arise in many physical contexts, such as shallow-water waves, ion-acoustic waves in plasmas, and others.[27,29–31] These asymptotic reductions allow us to construct approximate soliton solutions of the original nonlocal system in a two-step process: first, stable plane wave solutions are found, which serve as the "background" on top of which soliton solutions, obeying the KP equations, are obtained. We thus derive approximate soliton solutions, in the form of line solitons, as well as lumps and ring soliton of the nonlocal NLS system.

Our approach resembles the one used for single-component nonlocal NLS equations, where similar soliton solutions where found.[32–34] We thus predict the existence of weak antidark solitons that are supported by the nonlocality. In addition, however, there is a key element in our case, namely the role of multicomponents. Indeed, we show that the second component in our case permits the emergence of antidark solitons in a parametric region that would not be accessible for the single-component system. Thus, the nonlocal multicomponent NLS system, much like the local multicomponent one, does permit the emergence of soliton structures that cannot be supported in the single-component system (see, e.g., Ref. 35 for a recent review). The organization of the presentation, as well as a brief description of our main results and findings, are as follows.

In Section 2, we introduce the nonlocal NLS system, which is assumed to exhibit a defocusing nonlinearity, and can describe –as mentioned above– the interaction between two optical beams of different frequencies in nonlocal media; the model is formulated so that it can directly apply to the case of doped nematic liquid crystals.[21,36,37] After presenting the continuous-wave (cw) solution and discussing its stability, in Section 3, we use a multiscale analysis to obtain asymptotic reductions of the model at hand. We thus derive the KP and Johnson's equations in the Cartesian and cylindrical geometry, respectively. It is found that both the KP-I and KP-II versions[27] of the KP equation are possible, depending on the degree of nonlocality. Specifically, if the nonlocality parameter of the system is larger (smaller) than a characteristic critical value –or, in other words, if nonlocality is relatively strong (weak)–then the KP is of KP-II (KP-I) type. In Section 4, we use the KP soliton solutions to find approximate solitons of the original nonlocal NLS system, which turn out to be either of the antidark- or the dark-soliton-type, for a strong or weak nonlocality (in the sense discussed above), respectively. We thus find antidark and dark stripe solitons, dark lump solitons, as well as ring dark and antidark solitons. Results of direct numerical simulations fully support the predictions of our analysis. Indeed, it is found that the predicted approximate soliton solutions of the nonlocal NLS evolve without any distortion following the dynamics of the effective KP models; furthermore, analytically predicted and numerically computed soliton velocities and decay rates (in the cylindrical case) are found to be in very good agreement. Finally, in Section 5, we present our conclusions and discuss possibilities for future work.

2 | MODEL AND LINEAR REGIME

As mentioned above, the nonlocal NLS model under consideration is motivated by the field of nonlinear optics. In this context, consider two polarized, coherent light beams of two different frequencies that evolve, along the z-direction, in a planar nonlinear cell, filled, for example, with a nematic liquid crystal.[38] Then, if u and v are the complex electric field envelopes of the two light beams, and φ is the perturbation of the nematic director angle from its static value, the dynamics of the system is described by the following nondimensional equations:[38,39]

$$iu_t + \frac{d_1}{2}\Delta u - 2g_1\varphi u = 0, \tag{1}$$

$$iv_t + \frac{d_2}{2}\Delta v - 2g_2\varphi u = 0, \tag{2}$$

$$\nu\Delta\varphi - 2q\varphi + 2(g_1|u|^2 + g_2|v|^2) = 0, \tag{3}$$

where subscripts denote partial derivatives, t plays the role of the propagation coordinate, while

$$\Delta \equiv \partial_x^2 + \partial_y^2, \quad \text{or} \quad \Delta \equiv \frac{1}{r}\partial_r(r\partial_r) + \frac{1}{r^2}\partial_\theta^2,$$

is the transverse Laplacian in Cartesian or cylindrical coordinates, respectively. Here, the coefficients $d_{1,2}$ and $g_{1,2}$ characterize, respectively, the diffraction and nonlinearity for the two frequencies. The relative sign between the diffraction coefficients $d_{1,2}$ and nonlinearity coefficients $g_{1,2}$ in Equations (1) and (2) determines the nature of the equation, namely focusing or defocusing, much like the case of the relative NLS. Note that, typically, nematics feature a focusing nonlinearity, but they can become defocusing upon inclusion of doping.[21] Finally, the parameter q relates to the energy of the static field that pretilts the nematic dielectric, while the nonlocality parameter ν measures the elasticity of the nematic liquid crystal. Note that large ν corresponds to a highly nonlocal response, while in the limit $\nu \to 0$, one obtains the local variant of the system, namely:

$$iu_t + \frac{d_1}{2}\Delta u - \frac{2g_1}{q}\left(g_1|u|^2 + g_2|v|^2\right)u = 0, \tag{4}$$

$$iv_t + \frac{d_2}{2}\Delta v - \frac{2g_2}{q}\left(g_1|u|^2 + g_2|v|^2\right)v = 0. \tag{5}$$

Below, we will focus on the case of the defocusing nonlinearity, and we will thus assume that all parameters involved in Equations (1)-(3) are positive. In addition, as we are interested in finding solutions of the above system in the form of dark or antidark solitons, we supplement the system (1)-(3) with the following nontrivial boundary conditions:

$$|u| \to \rho_0, \quad |v| \to \sigma_0, \quad \varphi \to \varphi_0, \quad \text{as} \quad x, y \to \pm\infty, \tag{6}$$

where ρ_0, σ_0 and φ_0 are real constants.

To proceed with our analysis, we introduce the Madelung transformation for the fields u and v, namely,

$$u = \rho^{1/2}\exp(i\phi), \quad v = \sigma^{1/2}\exp(i\psi),$$

where real functions $\rho = \rho(\boldsymbol{r}, t)$, $\phi = \phi(\boldsymbol{r}, t)$ and $\sigma = \sigma(\boldsymbol{r}, t)$, $\psi = \psi(\boldsymbol{r}, t)$ denote amplitudes and phases, respectively; here, $\boldsymbol{r} = (x, y)$ or $\boldsymbol{r} = (r, \theta)$ for the Cartesian or the cylindrical setting. Then, Equations (1)-(3) reduce to the following hydrodynamic form:

$$\rho_t + d_1\nabla\cdot(\rho\nabla\phi) = 0, \tag{7}$$

$$\phi_t + 2g_1\varphi + \frac{d_1}{2}\left(|\nabla\phi|^2 - \rho^{-1/2}\Delta\rho^{1/2}\right) = 0, \tag{8}$$

$$\sigma_t + d_2\nabla\cdot(\sigma\nabla\psi) = 0, \tag{9}$$

$$\psi_t + 2g_2\varphi + \frac{d_2}{2}\left(|\nabla\psi|^2 - \sigma^{-1/2}\Delta\sigma^{1/2}\right) = 0, \tag{10}$$

$$\nu\Delta\varphi - 2q\varphi + 2(g_1\rho + g_2\sigma) = 0, \tag{11}$$

where $\nabla = (\partial_x, \partial_y)$ or $\nabla = (\partial_r, \frac{1}{r}\partial_\theta)$ is the gradient operator in Cartesian and cylindrical geometry, respectively. It is now observed that the simplest nontrivial solution of the above system, satisfying the boundary conditions (6), is

$$\rho = \rho_0, \quad \phi = -2g_1\varphi_0 t, \tag{12}$$

$$\sigma = \sigma_0, \quad \psi = -2g_2\varphi_0 t, \tag{13}$$

$$\varphi = \varphi_0 \equiv \frac{1}{q}(g_1\rho_0 + g_2\sigma_0), \tag{14}$$

where ρ_0 and σ_0 are real constants, as before. The above solution is, in fact, a continuous-wave (cw) for the fields u and v which, together with the constant function $\varphi = \varphi_0$, constitute what we call the background solution of Equations (1)-(3).

The stability analysis of the above background solution—which will serve as a "pedestal" of the soliton solutions—can be performed upon introducing in Equations (7)-(10) the perturbation ansatz:

$$\begin{aligned}
&\rho = \rho_0 + \varepsilon\tilde{\rho}, \quad \phi = -2g_1\varphi_0 t + \varepsilon\tilde{\phi},\\
&\sigma = \sigma_0 + \varepsilon\tilde{\sigma}, \quad \psi = -2g_2\varphi_0 t + \varepsilon\tilde{\psi},\\
&\varphi = \varphi_0 + \varepsilon\tilde{\varphi},
\end{aligned} \tag{15}$$

where ε is a small parameter ($0 < \varepsilon \ll 1$). Substituting Equations (15) into Equations (7)-(11), and keeping only the leading-order terms in ε, we obtain the following linear system:

$$\tilde{\rho}_t + d_1\rho_0\Delta\tilde{\phi} = 0, \tag{16}$$

$$\tilde{\phi}_t + 2g_1\tilde{\varphi} - \frac{d_1}{4\rho_0}\Delta\tilde{\rho} = 0, \tag{17}$$

$$\tilde{\sigma}_t + d_2\sigma_0\Delta\tilde{\psi} = 0, \tag{18}$$

$$\tilde{\psi}_t + 2g_2\tilde{\varphi} - \frac{d_2}{4\sigma_0}\Delta\tilde{\sigma} = 0, \tag{19}$$

$$\nu\Delta\tilde{\varphi} - 2q\tilde{\varphi} + 2(g_1\tilde{\rho} + g_2\tilde{\sigma}) = 0. \tag{20}$$

Next, we assume that the perturbations $\tilde{\rho}$, $\tilde{\phi}$, $\tilde{\upsilon}$, $\tilde{\varphi}$ are $\sim \exp[i(\boldsymbol{k}\cdot\boldsymbol{r} - \omega t)]$; here, $\boldsymbol{k} \equiv (k_x, k_y)$ and ω are the wave vector and frequency of the perturbation, respectively, and $\boldsymbol{r} \equiv (x, y)$. Then, Equations (16)-(20) lead to the dispersion relation:

$$p_1(k)\omega^4 + p_2(k)\omega^2 + p_3(k) = 0, \tag{21}$$

where the polynomials $p_j(k)$ $(j = 1, 2, 3)$ are given by

$$p_1(k) = 16(\nu k^2 + 2q), \tag{22}$$

$$p_2(k) = -4\nu \left(d_1^2 + d_2^2\right) k^6 - 8q \left(d_1^2 + d_2^2\right) k^4 - 64 \left(d_1 g_1^2 \rho_0 + d_2 g_2^2 \sigma_0\right) k^2, \tag{23}$$

$$p_3(k) = d_1^2 d_2^2 \nu k^{10} + 2d_1^2 d_2^2 q k^8 + 16 d_1 d_2 \left(d_2 g_1^2 \rho_0 + d_1 g_2^2 \sigma_0\right). \tag{24}$$

and $k^2 = k_x^2 + k_y^2$. It can be shown[40] that the system is modulationally stable, that is, the dispersion relation (21) has real roots, as long as the signs of the diffraction and nonlinearity coefficients are the same (in the context of our notation); this obviously corresponds to the defocusing case that we consider herein. Note that, clearly, this result does not depend on the coordinate system (Cartesian or cylindrical).

3 | NONLINEAR REGIME: KP AND JOHNSON'S EQUATIONS

Next, we proceed by analyzing Equations (7)-(11) via a multiscale expansion method in both Cartesian and cylindrical coordinates. This will lead to the derivation of an effective KP equation (for each geometry), the solutions of which will be exploited for the derivation of soliton solutions of the original nonlocal NLS system.

We seek solutions on top of the background solution (14) in the form of the following asymptotic expansions in ε:

$$\rho = \rho_0 + \varepsilon\rho_1 + \varepsilon^2\rho_2 + \cdots, \tag{25}$$

$$\phi = -2g_1\varphi_0 t + \varepsilon^{1/2}\phi_1 + \varepsilon^{3/2}\phi_2 + \cdots, \tag{26}$$

$$\sigma = \sigma_0 + \varepsilon\sigma_1 + \varepsilon^2\sigma_2 + \cdots, \tag{27}$$

$$\psi = -2g_2\varphi_0 t + \varepsilon^{1/2}\psi_1 + \varepsilon^{3/2}\psi_2 + \cdots, \tag{28}$$

$$\varphi = \varphi_0 + \varepsilon\varphi_1 + \varepsilon^2\varphi_2 + \cdots, \tag{29}$$

where the unknown fields $\rho_j, \phi_j, \varphi_j, \sigma_j$ and ψ_j (with $j = 1, 2, \ldots$) depend on the slow variables:

$$X = \varepsilon^{1/2}(x - ct), \quad Y = \varepsilon y, \quad T = \varepsilon^{3/2} t, \tag{30}$$

or

$$R = \varepsilon^{1/2}(r - ct), \quad \Theta = \varepsilon^{-1/2}\theta, \quad T = \varepsilon^{3/2}t, \tag{31}$$

for the Cartesian and cylindrical coordinates, respectively; here, c is the velocity of linear plane waves propagating on top of the background solution (so-called "speed of sound"). Note that, according to the original boundary conditions (6), the unknown fields must satisfy $\rho_j,\ \phi_j,\ \varphi_j, \sigma_j, \psi_j \to 0$ as $X, Y \to \infty$. Substituting Equations (25)-(29) into Equations (7)-(11), and using the variables (30) or (31), we obtain the following hierarchy of equations.

3.1 | Cartesian case

First, Equation (7) yields

$$O(\varepsilon^{3/2}) : -c\rho_{1X} + d_1\rho_0\phi_{1XX} = 0, \tag{32}$$

$$O(\varepsilon^{5/2}) : \quad \rho_{1T} - c\rho_{2X} + d_1\left[(\rho_1\phi_{1X})_X + \rho_0\phi_{1YY} + \rho_0\phi_{2XX}\right] = 0. \tag{33}$$

From Equation (8), we obtain

$$O(\varepsilon) : -c\phi_{1X} + 2g_1\varphi_1 = 0, \tag{34}$$

$$O(\varepsilon^2) : \phi_{1T} - c\phi_{2X} + 2g_1\varphi_2 + \frac{d_1}{2}\left(\phi_{1X}^2 - \frac{1}{2\rho_0}\rho_{1XX}\right) = 0. \tag{35}$$

Equation (9) yields

$$O(\varepsilon^{3/2}) : -c\sigma_{1X} + d_2\sigma_0\psi_{1XX} = 0, \tag{36}$$

$$O(\varepsilon^{5/2}) : \sigma_{1T} - c\sigma_{2X} + d_2\left[(\sigma_1\psi_{1X})_X + \sigma_0\phi_{1YY} + \sigma_0\psi_{2XX}\right] = 0. \tag{37}$$

From Equation (10), we obtain

$$O(\varepsilon) : -c\psi_{1X} + 2g_2\varphi_1 = 0, \tag{38}$$

$$O(\varepsilon^2) : \psi_{1T} - c\psi_{2X} + 2g_2\varphi_2 + \frac{d_2}{2}\left(\psi_{1X}^2 - \frac{1}{2\sigma_0}\sigma_{1XX}\right) = 0, \tag{39}$$

and, finally, Equation (11) leads to

$$O(\varepsilon) : -q\varphi_1 + g_1\rho_1 + g_2\sigma_1 = 0, \tag{40}$$

$$O(\varepsilon^2) : \nu\varphi_{1XX} - 2q\varphi_2 + 2(g_1\rho_2 + g_2\sigma_2) = 0. \tag{41}$$

Having set up the system of the above equations we now proceed by solving it consistently. First, consider the linear Equations (32), (34), (36), (38), and (40). This system can be simplified as follows: differentiate Equations (34) and (38) with respect to X, and substitute φ_1 from Equation (40), ϕ_{1XX} from Equation (32), and ψ_{1XX} from Equation (36). This yields the following two equations:

$$\left(-\frac{c^2}{d_1\rho_0} + \frac{2g_1^2}{q}\right)\rho_{1X} + \frac{2g_1g_2}{q}\sigma_{1X} = 0, \tag{42}$$

$$\left(-\frac{c^2}{d_2\sigma_0} + \frac{2g_2^2}{q}\right)\sigma_{1X} + \frac{2g_1g_2}{q}\rho_{1X} = 0. \tag{43}$$

The compatibility condition of Equations (42) and (43) is found by requiring the determinant of the coefficients to be zero. This leads to the determination of the speed of sound:

$$c^2 = \frac{2}{q}\left(d_1g_1^2\rho_0 + d_2g_2^2\sigma_0\right), \tag{44}$$

as well as to the following equation connecting the fields ρ_1 and σ_1:

$$\rho_{1X} = \frac{d_1g_1\rho_0}{d_2g_2\sigma_0}\sigma_{1X}. \tag{45}$$

Next, we proceed with the equations at the next order of approximation, namely with Equations (33), (35), (37), (39), and (41). First, multiply (35) by $\frac{d_1\rho_0}{c}$ and (39) by $\frac{d_2\sigma_0}{c}$, respectively, and differentiate them with respect to X. Then, adding the resulting equations with (33) and (37), respectively, we obtain the following system of equations:

$$\begin{aligned} &-c\rho_{2X} + \rho_{1T} + d_1(\rho_1\phi_{1X})_X + d_1\rho_0\phi_{1YY} + \frac{d_1\rho_0}{c}\phi_{1TX} + \frac{2d_1g_1\rho_0}{c}\varphi_{2X} \\ &+ \frac{d_1^2\rho_0}{2c}(\phi_{1X})_X^2 - \frac{d_1^2}{4c}\rho_{1XXX} = 0, \end{aligned} \tag{46}$$

$$\begin{aligned} &-c\sigma_{2X} + \sigma_{1T} + d_2(\sigma_1\psi_{1X})_X + d_2\sigma_0\psi_{1YY} + \frac{d_2\sigma_0}{c}\psi_{1TX} \\ &+ \frac{2d_2g_2\sigma_0}{c}\varphi_{2X} + \frac{d_2^2\sigma_0}{2c}(\psi_{1X})_X^2 - \frac{d_2^2}{4c}\sigma_{1XXX} = 0, \end{aligned} \tag{47}$$

$$\nu\varphi_{1XX} - 2q\varphi_2 + 2(g_1\rho_2 + g_2\sigma_2) = 0. \tag{48}$$

This system can be further simplified as follows. Multiply Equations (46) and (47) by $-\frac{g_1}{qc}$ and $-\frac{g_2}{qc}$, respectively, and add the resulting equations. Then, substitute φ_2 from Equation (48), and use $\phi_{1X} = \frac{c}{d_1\rho_0}\rho_1$, $\psi_{1X} = \frac{c}{d_2\sigma_0}\sigma_1$ and $\rho_{1X} = \frac{d_1 g_1 \rho_0}{d_2 g_2 \sigma_0}\sigma_{1X}$. This way, we end up with the following KP equation:

$$(\rho_{1T} + A_1\rho_{1XXX} + A_2\rho_1\rho_{1X})_X + \frac{c}{2}\rho_{1YY} = 0, \tag{49}$$

where the coefficients A_1 and A_2 are given by

$$A_1 = \frac{\nu c^4 - (d_1^3 g_1^2 \rho_0 + d_2^3 g_2^2 \sigma_0)}{4qc^3}, \tag{50}$$

$$A_2 = \frac{3(g_1^3 d_1^2 \rho_0 + g_2^3 d_2^2 \sigma_0)}{cd_1 g_1 \rho_0 q}. \tag{51}$$

Importantly, the above analysis ends up with a *single* KP equation for the unknown field ρ_1. Once this function assumes the form of a KP soliton, the unknown field σ_1 can be obtained from Equation (45), while the phases ϕ_1 and ψ_1 can be obtained from Equations (32) and (36), respectively. This way, as we will see, an approximate solution of the original nonlocal NLS system can be constructed upon employing the exact soliton solutions of the KP equation (49).

3.2 | Cylindrical case

In this case, Equations (7)-(11) lead to the following results. First, Equation (7) yields

$$O(\varepsilon^{3/2}) : -c\rho_{1R} + d_1\rho_0\phi_{1RR} = 0, \tag{52}$$

$$O(\varepsilon^{5/2}) : \rho_{1T} + d_1\left[(\rho_1\phi_{1R})_R + \frac{\rho_0}{c^2T^2}\phi_{1\Theta\Theta} + \frac{\rho_0}{cT}\phi_{1R} + \rho_0\phi_{2RR}\right] \tag{53}$$

with $-c\rho_{2R} = 0$. From Equation (8) we obtain

$$O(\varepsilon) : -c\phi_{1R} + 2g_1\varphi_1 = 0, \tag{54}$$

$$O(\varepsilon^2) : \phi_{1T} - c\phi_{2R} + 2g_1\varphi_2 + \frac{d_1}{2}\left(\phi_{1R}^2 - \frac{1}{2\rho_0}\rho_{1RR}\right) = 0. \tag{55}$$

Equation (9) yields

$$O(\varepsilon^{3/2}) : -c\sigma_{1R} + d_2\sigma_0\psi_{1RR} = 0, \tag{56}$$

$$O(\varepsilon^{5/2}) : \sigma_{1T} + d_2\left[(\sigma_1\psi_{1R})_R + \frac{\sigma_0}{c^2T^2}\psi_{1\Theta\Theta} + \frac{\sigma_0}{cT}\psi_{1R} + \sigma_0\psi_{2RR}\right] \tag{57}$$

with $-c\sigma_{2R}=0$. From Equation (10) we obtain

$$O(\varepsilon):\ -c\psi_{1R}+2g_2\varphi_1=0, \tag{58}$$

$$O(\varepsilon^2):\ \psi_{1T}-c\psi_{2R}+2g_2\varphi_2+\frac{d_2}{2}\left(\psi_{1R}^2-\frac{1}{2\sigma_0}\sigma_{1RR}\right)=0, \tag{59}$$

and Equation (11) leads to

$$O(\varepsilon):\ -q\varphi_1+g_1\rho_1+g_2\sigma_1=0, \tag{60}$$

$$O(\varepsilon^2):\ \nu\varphi_{1RR}-2q\varphi_2+2(g_1\rho_2+g_2\sigma_2)=0. \tag{61}$$

The above system can be solved using the methodology presented in the Cartesian case. We thus end up with the following cylindrical KP equation, also known as Johnson's equation:[28]

$$\left(\rho_{1T}+A_1\rho_{1RRR}+A_2\rho_1\rho_{1R}+\frac{1}{2T}\rho_1\right)_R+\frac{1}{2cT^2}\rho_{1\Theta\Theta}=0, \tag{62}$$

where the coefficients A_1 and A_2 are given by Equations (50) and (51). As in the Cartesian case, solutions of the Johnson's equation (62) can be used to obtain approximate solutions of the non-local NLS system.

3.3 | Versions of the KP and Johnson's equations

Having derived the KP and Johnson's equations, for the Cartesian and cylindrical geometry, respectively, it is convenient to further normalize these equations and express them in their "standard" form.[2,29] We begin with the Cartesian case, namely with the KP equation (49). We introduce the transformations:

$$T\mapsto A_1T,\quad Y\mapsto\sqrt{\frac{6|A_1|}{c}}Y,\quad \rho_1\mapsto\frac{A_2}{6A_1}\rho_1, \tag{63}$$

and put Equation (49) into the form:

$$(\rho_{1T}+\rho_{1XXX}+6\rho_1\rho_{1X})_X+3\sigma\rho_{1YY}=0, \tag{64}$$

where

$$\sigma=\mathrm{sgn}(A_1). \tag{65}$$

Similarly, in the cylindrical case, we use the scale transformations:

$$T\mapsto A_1T,\quad \Theta\mapsto\sqrt{\frac{6c}{|A_1|}}\Theta,\quad \rho_1\mapsto\frac{A_2}{6A_1}\rho_1, \tag{66}$$

and cast Johnson's equation (62) into the form:

$$\left(\rho_{1T} + \rho_{1RRR} + 6\rho_1\rho_{1R} + \frac{1}{2T}\rho_1\right)_R + \frac{3\sigma}{T^2}\rho_{1\Theta\Theta} = 0, \tag{67}$$

where σ is given by Equation (65).

According to the above, it is clear that the type of KP equation—either in Cartesian or cylindrical coordinates—is determined by the parameter σ, that is, the sign of parameter A_1: For $\sigma = +1$ ($A_1 > 0$), the KP equations are of KP-II type, while for $\sigma = -1$ ($A_1 < 0$) the KP equations are of KP-I type. It is important to point out that—as we will see below—the parameter σ not only characterizes the type of the equation (and the stability of its soliton solutions), but also the type of soliton itself, which may be of the dark or bright type (on top of the background solution). Note that the value of σ turns out to depend on the degree of nonlocality—see below.

4 | APPROXIMATE SOLITON SOLUTIONS

The above multiscale analysis reveals that one can construct approximate (i.e., valid up to order $O(\varepsilon)$) soliton solutions of the nonlocal NLS system (1)-(3). This solution can be expressed in terms of the soliton solution ρ_1 of the KP equations (49) or (62), in the Cartesian and cylindrical geometry, respectively, as follows:

$$u \approx (\rho_0 + \varepsilon\rho_1)^{1/2} \exp\left[-2ig_1\varphi_0 t + i\varepsilon^{1/2}\frac{c}{d_1\rho_0}\int \rho_1 \mathrm{d}\xi\right], \tag{68}$$

$$v \approx \left(\sigma_0 + \varepsilon\frac{d_2 g_2\sigma_0}{d_1 g_1\rho_0}\rho_1\right)^{1/2} \exp\left[-2ig_2\varphi_0 t + i\varepsilon^{1/2}\frac{cg_2}{d_1 g_1\rho_0}\int \rho_1 \mathrm{d}\xi\right], \tag{69}$$

$$\varphi \approx \varphi_0 + \varepsilon\frac{g_1}{q}\left(1 + \frac{d_2 g_2^2\sigma_0}{d_1 g_1^2\rho_0}\right)\rho_1, \tag{70}$$

where $\xi = X$ or $\xi = R$ for the Cartesian or the cylindrical geometry, respectively. Here, it is reminded that ρ_0 and σ_0 are arbitrary $O(1)$ parameters that set the background amplitudes, while φ_0 is given in Equation (14). Next, we will proceed to identify the types of these approximate soliton solutions, and study their dynamics via direct numerical simulations.

4.1 | Cartesian case

4.1.1 | Antidark and dark stripe solitons

We start with the KP in Cartesian coordinates, namely Equation (49). The simplest soliton solution of this equation is the line soliton, which is actually a tilted KdV soliton in the xy-plane. The relevant one-line soliton solution of Equation (49) reads

$$\rho_1 = \frac{12A_1}{A_2}\kappa^2 \mathrm{sech}^2\xi, \tag{71}$$

$$\xi \equiv \kappa\left[X + \lambda\sqrt{\frac{6|A_1|}{c}}Y - A_1\left(4\kappa^2 + 3\lambda^2\right)T + \delta_0\right], \tag{72}$$

where the free, $O(1)$, parameters κ and λ control the propagation direction in the plane, and δ_0 sets the initial soliton location. Using Equations (50) and (51), it can readily be found that the soliton amplitude is given by

$$\frac{12A_1}{A_2}\kappa^2 = (\nu - \nu_c)\frac{c^2 d_1 g_1 \rho_0}{d_1^3 g_1^2 \rho_0 + d_2^3 g_2^2 \sigma_0}\kappa^2, \tag{73}$$

where the critical value ν_c is given by

$$\nu_c = \frac{1}{c^4}\left(d_1^3 g_1^2 \rho_0 + d_2^3 g_2^2 \sigma_0\right). \tag{74}$$

It is now important to note that as the fraction in the right-hand side of Equation (73) is always positive, the type of the soliton of Equation (49) depends crucially on the sign of $\nu - \nu_c$. In addition, it is easy to see that

$$\mathrm{sgn}(\sigma) = \mathrm{sgn}(\nu - \nu_c), \tag{75}$$

which means that both the type of the KP equation and the stability of its line soliton solution depend on the degree of nonlocality. In particular:

- If $\nu > \nu_c$ ($\sigma = +1$), that is, for a relatively *strong nonlocality*, Equation (49) is of the KP-II type, and its line soliton solution (71) gives rise to *antidark* stripe solitons (see Equations (68)-(69)), namely of the form of intensity elevations on top of the cw background.
- If $\nu < \nu_c$ ($\sigma = -1$), that is, for a relatively *weak nonlocality* (in other words, closer to the local NLS limit—see Equations (4)-(5)), Equation (49) is of the KP-I type and its line soliton solution (71) leads to approximate *dark* soliton stripes (see Equations (68)-(69)), that is, intensity dips off of the cw background.

It is clear from Equations (50), (51), and (73) that the type of the soliton (dark or antidark) depends on the sign of the coefficient A_1. The latter is depicted in Figure 1 as a function of the nonlocality parameter ν for both the one- (red line) and the two-component (blue line) cases. Other parameter values are fixed, namely $d_1 = g_1 = q/5 = 1$ for the one-component system, $d_1 = 2d_2/3 = g_1 = g_2 = q/5 = 1$, for the two-component one, while, in both cases, the cw amplitudes are chosen as $\rho_0 = \sigma_0 = 1$. Shown also are the regimes of existence of dark and antidark solitons: in the one- (two-) component system, dark solitons exist for $\nu < \nu_1$ ($\nu < \nu_2$), while antidark ones exist for $\nu > \nu_1$ ($\nu > \nu_2$). It is thus clear that the role of the second component is to reduce the threshold set by the nonlocality parameter for the existence of antidark solitons: indeed, these states can be formed in the interval $\nu_1 < \nu < \nu_2$, which would not be possible in the single-component system.

The existence and dynamics of these approximate soliton solutions will be investigated below by means of direct simulations. Nevertheless, before proceeding, it is important to make the following comments. As is well known (see, e.g., Refs. 25, 41 and references therein), the line

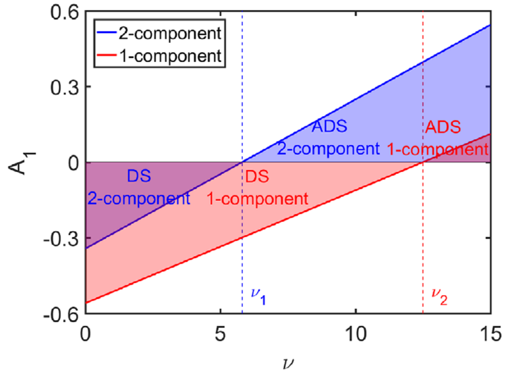

FIGURE 1 The possible type of solitons (dark or antidark) in the (A_1, ν) plane, for both cases of the single- (red line) and two- (blue line) component systems. Observe that the role of the second component in the two-component system is to reduce the threshold set by the nonlocality parameter ν for the existence of antidark solitons (see text)

soliton solutions of the KP-II (KP-I) are stable (unstable) under the action of long-wavelength transverse perturbations; in such a situation, the line soliton develop strong undulations and eventually decay—see, for example, the review[25] for analysis and references therein, as well as Ref. 42 for results of numerical simulations. However, as was recently shown,[26] the effect of nonlocality can suppress the transverse instability, in the sense that it manifests itself at later times compared to the local NLS case. It is therefore relevant to investigate not only the antidark stripe solitons, but also the dark ones, which may also exist and propagate for finite times in the nonlocal system.

In what follows, we will use the exponential time-differencing fourth-order Runge-Kutta (ETDRK4) method of Ref. 43 to verify that the above solutions do propagate as solutions of the original nonlocal NLS model. In particular, we use initial conditions of the form $u(x, y, 0) = u_b(x, y)u_s(x, y, 0)$ (and similarly for the field v), where $u_s(x, y, 0)$ is the initial soliton profile (i.e., the solution (68) at $t = 0$). Furthermore, $u_b(x, y)$ is an almost flat background of finite extent (in the infinite system, this would be $u_b(x, y) = 1$), namely a very broad super-Gaussian of the form $u_b(x, y) = \exp[-(x/0.8L)^{12} - (y/0.8L)^{12}]$, where $x, y \in [-L, L]$; here, L denotes the size of the computational domain, taken to be sufficiently large (e.g., of the order of 10^3). Note that the use of a background of finite extent is more realistic, as dark (or antidark) solitons are always created on top of a finite background in real experiments. Then, using these initial conditions ($t = 0$), we numerically integrate the nonlocal NLS system (1)-(3) with the following choices for the parameter values:

$$d_1 = 2d_2/3 = g_1 = g_2 = \nu/5 = q/5 = 1, \quad \rho_0 = \sigma_0 = 1, \tag{76}$$

and for the soliton parameters $\lambda = \delta_0 = 0$ and $\kappa = 1$. Note that this choice gives $A_1 = 1/32 > 0$, $A_2 = 39/20 > 0$, and $\nu_c = 35/8 < \nu$ (i.e., $\sigma = +1$), which means that the solitons are of the antidark type and the amplitude function ρ_1 obeys the KP-II equation. For the above choice, the initial condition for our direct simulations, which depends only on the formal small parameter ε, reads:

$$u(x, y, 0) = \sqrt{1 + \frac{5}{26}\varepsilon\,\mathrm{sech}^2(\varepsilon^{1/2}x)}\,\exp\left[i\frac{5}{26}\varepsilon^{1/2}\tanh(\varepsilon^{1/2}x)\right], \tag{77}$$

$$v(x,y,0)=\sqrt{1+\frac{15}{52}\varepsilon\,\mathrm{sech}^2(\varepsilon^{1/2}x)}\exp\left[i\frac{5}{26}\varepsilon^{1/2}\tanh(\varepsilon^{1/2}x)\right], \tag{78}$$

$$\varphi(x,y,0)=\frac{2}{5}+\frac{5}{52}\varepsilon\,\mathrm{sech}^2(\varepsilon^{1/2}x), \tag{79}$$

and we fix $\varepsilon = 0.1$. The propagation, depicted in Figure 2, shows that the antidark stripes do exist and propagate without any distortion up to time $t = 50$.

A similar situation occurs also for the approximate dark soliton stripe solitons, for which the field ρ_1 obeys the KP-I equation. To show this, first we note that, for the following choice of the parameter values:

$$d_1 = 2d_2/3 = g_1 = g_2 = \nu = q/5 = 1, \quad \rho_0 = \sigma_0 = 1, \tag{80}$$

and for soliton parameters $\lambda = \delta_0 = 0$ and $\kappa = 1$ as before, one obtains $A_1 = -27/160 < 0$, $A_2 = 39/20$, and $\nu_c = 35/8 > \nu = 1$ (i.e., $\sigma = -1$), which corresponds to the case of dark solitons. For these parameter values, the initial conditions are

$$u(x,y,0)=\sqrt{1-\frac{27}{26}\varepsilon\,\mathrm{sech}^2(\varepsilon^{1/2}x)}\exp\left[-i\frac{27}{26}\varepsilon^{1/2}\tanh(\varepsilon^{1/2}x)\right], \tag{81}$$

$$v(x,y,0)=\sqrt{1-\frac{81}{52}\varepsilon\,\mathrm{sech}^2(\varepsilon^{1/2}x)}\exp\left[-i\frac{27}{26}\varepsilon^{1/2}\tanh(\varepsilon^{1/2}x)\right], \tag{82}$$

$$\varphi(x,y,0)=\frac{2}{5}-\frac{27}{52}\varepsilon\,\mathrm{sech}^2(\varepsilon^{1/2}x). \tag{83}$$

The results of the direct simulations, stemming from the above initial condition for $\varepsilon = 0.1$ (as in the antidark soliton case), are shown in Figure 3. It can readily be seen that dark solitons stripes are also supported by the original nonlocal system and, interestingly, can propagate undistorted up to $t = 50$. Thus, although these structures obey an effective KP-I equation—and, as such, should be prone to transverse instability—they do feature a stable evolution for finite times; this is in accordance with the analysis of Ref. 26, predicting nonlocality-induced partial suppression of the transverse instability. We note in passing that we have checked that, indeed, at later times the transverse instability sets in and eventually destroys the dark soliton stripes. A systematic investigation of such an analysis, which is relevant and interesting in its own right, is beyond the scope of this work.

At this point, it is also relevant to test the validity of our analytical approximations, by comparing the numerical and analytical values of the solitons' velocities. In particular, according to our analytical approximation, the stripe solitons propagate with a velocity $v_s = c + 4\varepsilon\kappa^2 A_1$. Using the above mentioned parameter values, we find that $v_s \approx 1.01$ for the antidark solitons, and $v_s \approx 0.93$ for the dark solitons. On the other hand, the respective numerical values $v_{\mathrm{num}} = \Delta x/\Delta t$ (where Δx is the distance traveled by the soliton in time Δt) are $v_{\mathrm{num}} \approx 1$ and $v_{\mathrm{num}} \approx 0.92$ for the antidark and dark soliton stripes, respectively. As one can see, the agreement between the analytical predictions and the numerical results is excellent.

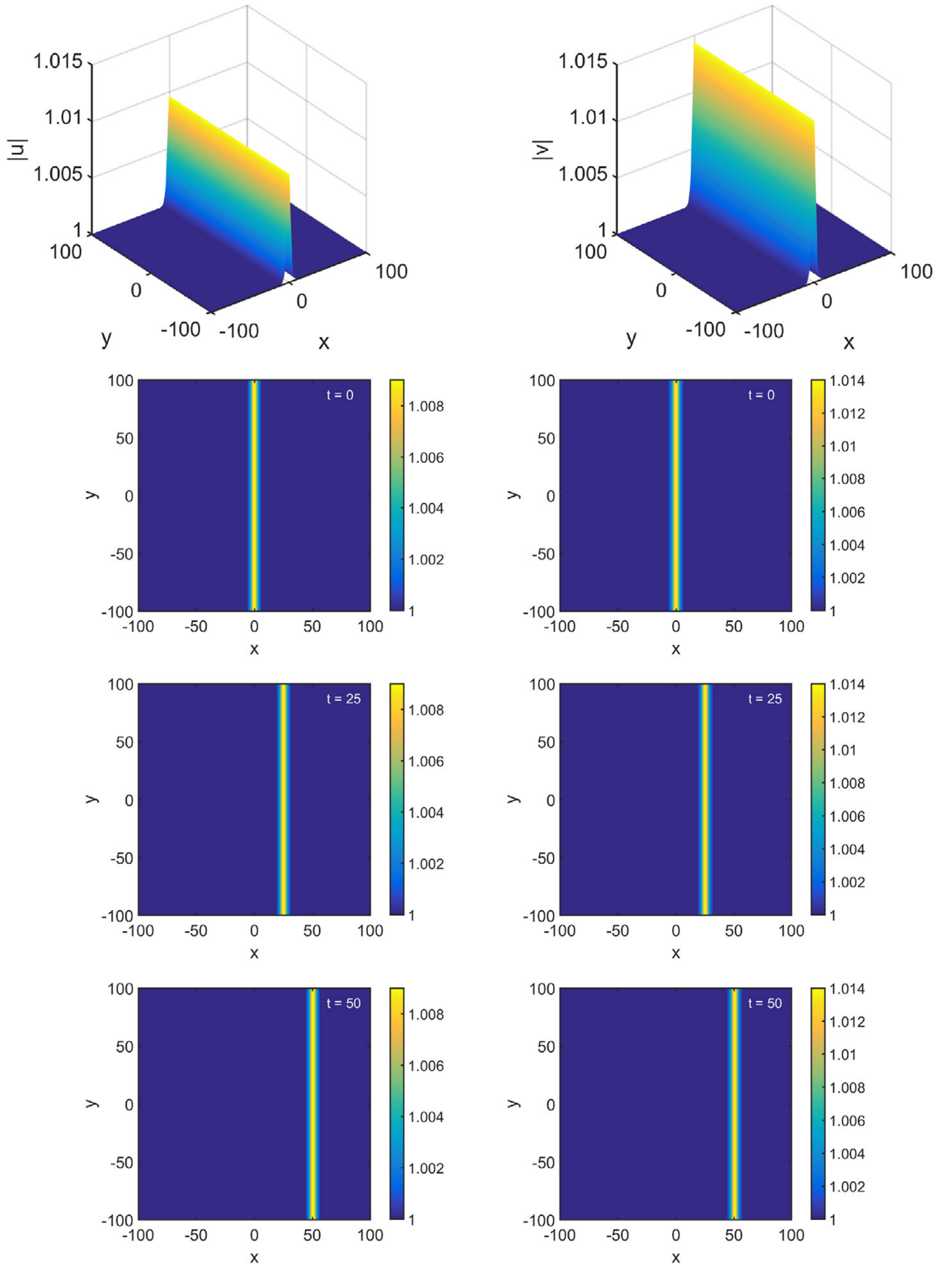

FIGURE 2 The two top panels show, in 3D, the spatial profile of the modulus of the antidark stripe solitons at $t = 0$—see Equations (77) and (78) with $\varepsilon = 0.1$. Left (right) panels depict the u- (v-)component, and the three bottom rows are contour plots showing the modulus of the antidark solitons at $t = 0$, $t = 25$ and $t = 50$

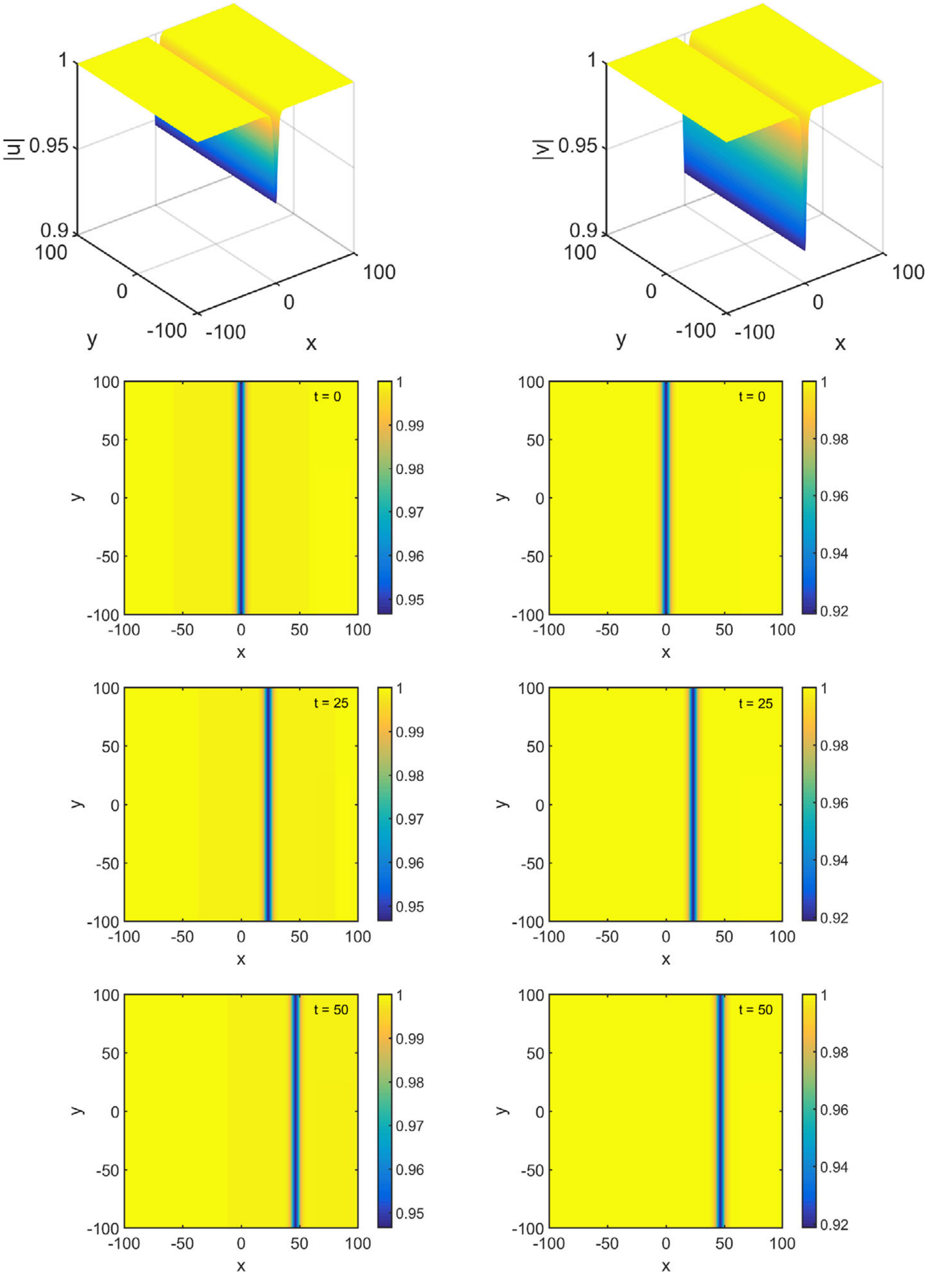

FIGURE 3 Similar to Figure 2, but for the case of dark stripe solitons. The initial condition, in this case, is given by Equations (81) and (82), for $\varepsilon = 0.1$

4.1.2 | Dark lump solitons

Apart for the 1D stripe soliton solutions that were studied before, the KP-I equation (for $A_1 < 0$, or $\sigma = -1$, corresponding to the weakly nonlocal regime) supports also genuinely 2D solitons. These states, known as "lumps," [2] are weakly localized—that is, they decay algebraically at infinity. A lump solution of Equation (49) is given by

$$\rho_1(X,Y,T) = \frac{24A_1}{A_2}\frac{-\frac{3A_1}{\alpha} - (X+\alpha T)^2 + \frac{2\alpha Y^2}{c}}{\left(-\frac{3A_1}{\alpha} + (X+\alpha T)^2 + \frac{2\alpha Y^2}{c}\right)^2}, \tag{84}$$

where α is a $O(1)$ free parameter linking the soliton amplitude with its velocity and transverse width. Note that, as here $\sigma = -1$, we have $A_1 < 0$, meaning that the vector soliton solution (68) and (69) is of the dark type; in other words, in this case, the approximate 2D soliton solutions supported by the nonlocal NLS system are *dark lumps*.

The existence and dynamics of these structures is also investigated numerically. In particular, choosing the same parameter values that were used in the case of the dark soliton stripe (see Equation (80)), and fixing $\alpha = 1$, the relevant initial condition that we use in the simulations is

$$u(x,y,0) = \sqrt{1 - \frac{27\varepsilon}{13}\frac{\frac{81}{160} - \varepsilon x^2 + 2\varepsilon^2 y^2}{\left(\frac{81}{160} + \varepsilon x^2 + 2\varepsilon^2 y^2\right)^2}} \times \exp\left(-i\frac{27}{13}\frac{\varepsilon x}{\frac{81}{160} + \varepsilon x^2 + 2\varepsilon^2 y^2}\right), \tag{85}$$

$$v(x,y,0) = \sqrt{1 - \frac{81\varepsilon}{26}\frac{\frac{81}{160} - \varepsilon x^2 + 2\varepsilon^2 y^2}{\left(\frac{81}{160} + \varepsilon x^2 + 2\varepsilon^2 y^2\right)^2}} \times \exp\left(-i\frac{27}{13}\frac{\varepsilon x}{\frac{81}{160} + \varepsilon x^2 + 2\varepsilon^2 y^2}\right), \tag{86}$$

$$\varphi(x,y,0) = \frac{2}{5} - \frac{27\varepsilon}{26}\frac{\frac{81}{160} - \varepsilon x^2 + 2\varepsilon^2 y^2}{\left(\frac{81}{160} + \varepsilon x^2 + 2\varepsilon^2 y^2\right)^2}. \tag{87}$$

The results of the simulations, for $\varepsilon = 0.1$ as before, is shown in Figure 4.

Once again, we find that our analytical predictions are numerically confirmed: the dark lumps do exist and propagate without any deformation, for times up to $t = 50$. Furthermore, as in the case of soliton stripes, we have compared analytical and numerical values of the lump velocity. The analytical prediction is $v_{\text{an}} = c - \varepsilon\alpha \approx 0.9$, the respective numerical value is $v_{\text{n}} = \Delta x/\Delta t \approx 0.88$; once again, we find an excellent agreement between the two.

Here, we should also mention that it is expected (as per the analysis of Refs. 23, 24, 44) that sufficiently weak dark soliton stripes, in the form of Equations (81)-(82), which undergo the transverse instability, will eventually decay into 2D structures that resemble dark lumps. As mentioned above, a detailed analysis of the instability induced dynamics of the dark soliton stripes is beyond the scope of this work. Interestingly, however, KP-I lumps were long conjectured to be stable (see, for instance,[45]) but no proof was available until recently. In Ref. 46, Bäcklund transformations are used to prove that the KP-I lump is nondegenerate, with Morse index 1 and, as a consequence, it is orbitally stable.

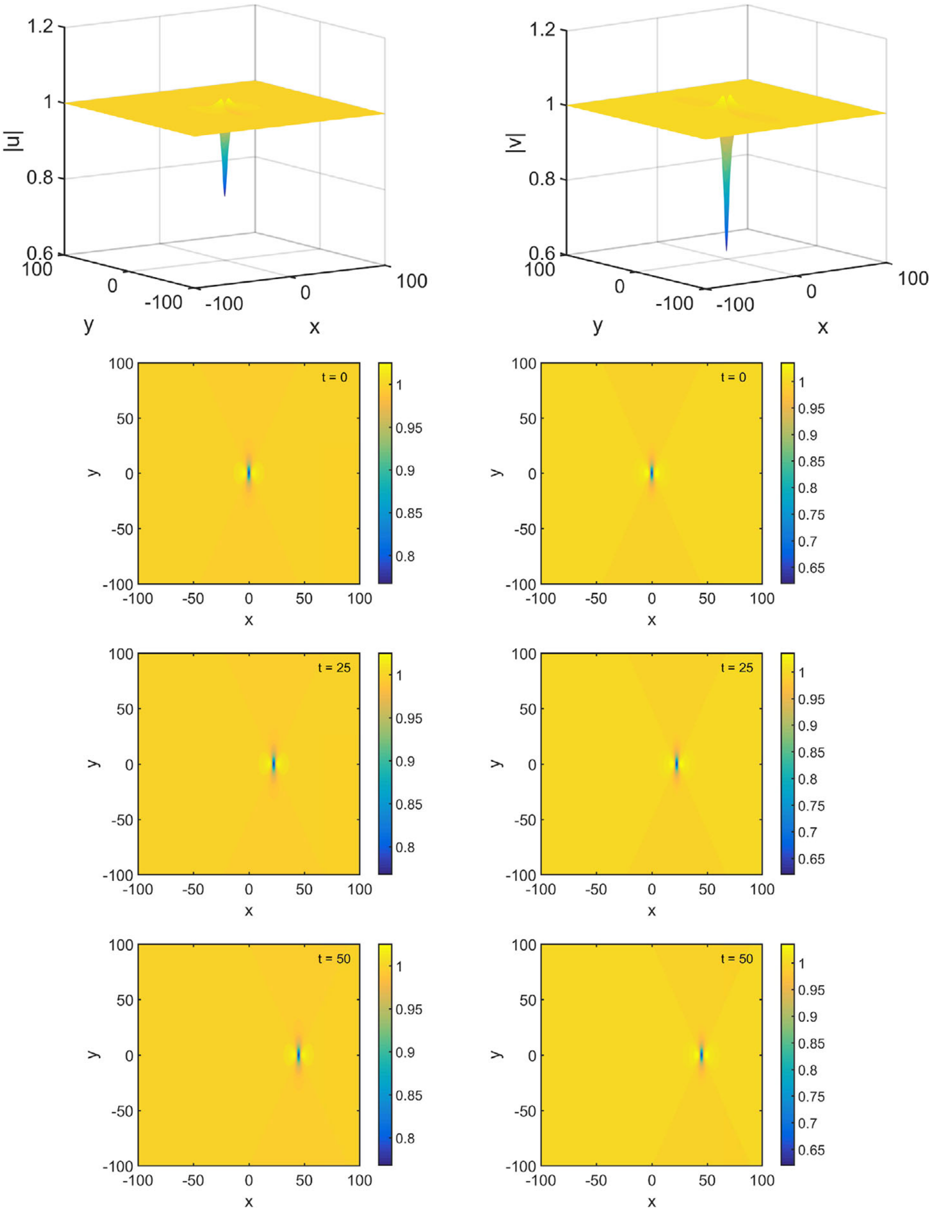

FIGURE 4 Similar to Figure 3, but now for the dark lump soliton. Here, the initial condition is given by Equations (85)-(86), for $\varepsilon = 0.1$

4.2 | Cylindrical case

Next, we proceed with the cylindrical case, and derive approximate soliton solutions governed by Johnson's equation (62), which—much like the Cartesian KP (49)—is a completely integrable model.[47] As for its soliton solutions, here we focus on radially symmetric solitons, which are independent of Θ. In this case, Johnson's equation reduces to the cylindrical KdV (cKdV) equation:

$$\rho_{1T} + A_1\rho_{1RRR} + A_2\rho_1\rho_{1R} + \frac{1}{2T}\rho_1 = 0, \tag{88}$$

which has cylindrical (sech^2-shaped) soliton solutions on top of a rational background.[48] Such soliton solutions of Equation (88) read:

$$\rho_1 = \frac{R}{2A_2T} + \frac{12\eta^2 A_1}{A_2}\left(\frac{T_0}{T}\right)\text{sech}^2\zeta, \tag{89}$$

$$\zeta \equiv \eta\left(\frac{T_0}{T}\right)^{1/2} R + A_1\left[2\eta\left(\frac{T_0}{T}\right)^{1/2}\right]^3 T + \zeta_0, \tag{90}$$

where η, T_0, and ζ_0 are free parameters. Let us now assume that $T \mapsto T + T_0$ (with $T_0 \gg T$), $R \mapsto R + R_0$ (with $R_0 \gg R$), and consider the regime $T_0 \gg R_0$. Then, it can readily be found that, in this limit, the solution (89) reduces to the usual KdV soliton:

$$\rho_1 \to \frac{12\eta^2 A_1}{A_2}\text{sech}^2\left[\eta\left(R - 4A_1\eta^2 T + \zeta_0\right)\right], \tag{91}$$

that is, Equation (89) becomes identical to Equation (71) for $\lambda = 0$, and with the obvious changes $\eta \mapsto \kappa$, as well as $X \mapsto R$ and $\delta_0 \mapsto \zeta_0$. Note that the rational background ($\propto R/T$) in Equation (89) does not play any role here, as we are considering the long-time behavior of solutions featuring large radii; for an analysis of the asymptotic behavior in the limit $t \to 0$, see Ref. 49.

It is clear that Equation (91) describes a ring-shaped soliton (which, in our case, is on top of the cw pedestal), characterized by the free parameter η, which sets the soliton characteristics. In particular, the parameters characterizing the soliton's core, that is, amplitude, power, velocity, and inverse width, scale according to η^2, η^3, η^4, and η, respectively, as is the case of usual KdV solitons. As concerns the type of the ring solitons, they are either antidark or dark. Specifically, the sign of A_1 determines, once again, the nature of the soliton: if $A_1/A_2 > 0$ (i.e., $\sigma = +1$ and $\nu > \nu_c$), the solitons are annular humps on top of the cw background, hence *ring anti-dark solitons* (RAS); if $A_1/A_2 < 0$ (i.e., $\sigma = -1$ and $\nu < \nu_c$), the solitons are annular depressions of the background, hence *ring dark solitons* (RDS).

Thus, an interesting question is what would happen if a sech^2 initial profile evolved under the cKdV, Eq. (88). The answer, which was found first numerically[50] and later analytically,[51,52] is that the solution of the relevant Cauchy problem consists of a primary wave, of a sech^2 profile, and a very small-amplitude shelf. Indeed, the asymptotic analysis of the cKdV equation, based on an appropriate small parameter ($\epsilon = 1/\text{initial radius}$, in dimensionless variables), shows the following:[51,52] to leading order of approximation, and in the regime $T \gg R$ (i.e., the first term in Equation (89) is much smaller than the second), the primary wave (that decays to zero at both upstream and downstream infinity) takes the form of the KdV soliton of Equation (91). Nevertheless, as indicated by Equations (89)-(90), there exists an important difference: η now becomes a slowly varying function of T, due to the presence of the term $(1/2T)\rho_1$ in the cKdV equation.

According to the above discussion, an approximate solution of Equations (1)-(3) in the cylindrical geometry is given by the primary part of the soliton (see Equation (91) and remarks above), with the soliton amplitude and velocity varying with time. To justify this, and investigate the propagation properties of RAS and RDS, we numerically evolve an initial (at $t = t_0 = 5$) annular profile for both cases. In other words, and as explained above, the initial conditions used in the simulations for the RAS are

$$u(x,y,5) = \sqrt{\frac{29}{39} + \frac{2}{39}\sqrt{x^2+y^2} - \frac{27}{130}\varepsilon^{-1/2}\mathrm{sech}^2\left[\frac{27}{20\sqrt{5}} - \frac{\varepsilon^{-1/4}}{\sqrt{5}}\left(\sqrt{x^2+y^2}-5\right)\right]}$$
$$\times \exp\left[-\frac{i}{39}\left(131-(x^2+y^2)+10\sqrt{x^2+y^2}\right)\right)$$
$$+\left(\left(\frac{27}{26\sqrt{5}}\varepsilon^{-1/4}\tanh\left[\frac{27}{20\sqrt{5}} - \frac{\varepsilon^{-1/4}}{\sqrt{5}}\left(\sqrt{x^2}+y^2-5\right)\right]\right)\right] \tag{92}$$

$$v(x,y,5) = \sqrt{\frac{8}{13} + \frac{1}{13}\sqrt{x^2+y^2} - \frac{81}{260}\varepsilon^{-1/2}\mathrm{sech}^2\left[\frac{27}{20\sqrt{5}} - \frac{\varepsilon^{-1/4}}{\sqrt{5}}\left(\sqrt{x^2+y^2}-5\right)\right]}$$
$$\times \exp\left[-\frac{i}{39}\left(131-(x^2+y^2)+10\sqrt{x^2+y^2}\right)\right)$$
$$+\left(\left(\frac{27}{26\sqrt{5}}\varepsilon^{-1/4}\tanh\left[\frac{27}{20\sqrt{5}} - \frac{\varepsilon^{-1/4}}{\sqrt{5}}\left(\sqrt{x^2}+y^2-5\right)\right]\right)\right] \tag{93}$$

$$\varphi(x,y,5) = \frac{53}{195} + \frac{1}{39}\sqrt{x^2+y^2} - \frac{27}{260}\varepsilon^{-1/2}\mathrm{sech}^2\left[\frac{27}{20\sqrt{5}} - \frac{\varepsilon^{-1/4}}{\sqrt{5}}\left(\sqrt{x^2+y^2}-5\right)\right] \tag{94}$$

while the initial conditions for the RDS read:

$$u(x,y,5) = \sqrt{\frac{29}{39} + \frac{2}{39}\sqrt{x^2+y^2} + 3\varepsilon^{-1/2}\mathrm{sech}^2\left[\frac{1}{4\sqrt{5}} + \frac{\varepsilon^{-1/4}}{\sqrt{5}}\left(\sqrt{x^2+y^2}+5\right)\right]}$$
$$\times \exp\left[-\frac{i}{39}\left(131-(x^2+y^2)\right)\right)$$
$$+\left(\left(10\sqrt{x^2+y^2} - 6\sqrt{5}\varepsilon^{-1/4}\tanh\left[\frac{1}{4\sqrt{5}} + \frac{\varepsilon^{-1/4}}{\sqrt{5}}\left(\sqrt{x^2}+y^2+5\right)\right]\right)\right] \tag{95}$$

$$v(x,y,5) = \sqrt{\frac{8}{13} + \frac{1}{13}\sqrt{x^2+y^2} + 3\varepsilon^{-1/2}\mathrm{sech}^2\left[\frac{1}{4\sqrt{5}} + \frac{\varepsilon^{-1/4}}{\sqrt{5}}\left(\sqrt{x^2+y^2}+5\right)\right]}$$
$$\times \exp\left[-\frac{i}{39}\left(131-(x^2+y^2)+10\sqrt{x^2+y^2}\right)\right)$$

$$-\left(\left(6\sqrt{5}\varepsilon^{-1/4}\tanh\left[\frac{1}{4\sqrt{5}}+\frac{\varepsilon^{-1/4}}{\sqrt{5}}\left(\sqrt{x^2}+y^2+5\right)\right]\right)\right] \tag{96}$$

$$\varphi(x,y,5)=\frac{53}{195}+\frac{1}{39}\sqrt{x^2+y^2}+\frac{1}{52}\varepsilon^{-1/2}\mathrm{sech}^2\left[\frac{1}{4\sqrt{5}}+\frac{\varepsilon^{-1/4}}{\sqrt{5}}\left(\sqrt{x^2+y^2}+5\right)\right] \tag{97}$$

where the initial radii are $r_0 = 4.6$ for the RAS and $r_0 = 7.37$ for the RDS, respectively. In the numerical simulations, we use the parameter values (76) and (80), for the RAS and RDS, respectively, as well as the value $\varepsilon = 0.1$.

The results of the simulations are shown in Figures 5 (for the RAS) and 6 (for the RDS). It is clearly observed that both structures undergo an expansion, without any distortion, which justifies the existence of these states, and supports our analytical prediction regarding their dynamics. Note that the expanding dynamics of the ring solitons can roughly be understood as the dynamics of a right-going stripe soliton of finite length, which is bent so as to form a ring soliton.

To further test the validity of our analytical approach, we have also calculated the analytical and numerical values of the ring solitons' velocities. The analytical prediction is $\upsilon_r = c - (1/2)\varepsilon^{1/2} r_0 t^{-1/2}$ leading to the values $\upsilon_r \approx 0.85$ for the RAS and $\upsilon_r \approx 0.9$ for the RDS. The respective numerically found velocities, $\upsilon_{\text{num}} = \Delta r/\Delta t$ (where Δr is the change of the soliton radius during the time Δt), are $\upsilon_n \approx 0.99$ for the RAS and $\upsilon_{\text{num}} \approx 1$ for the RDS, in reasonably good agreement with the analytical predictions. In addition, in this case, it is relevant to estimate analytical and numerical decay rates. Using Equation (89), the analytical estimation for the decay rate is $(t_0/t) = 5/50 = 0.1$, while the numerically found decay rate for the RAS and RDS is given by ≈ 0.098, as seen in Figures 5 (for the RAS) and 6 (for the RDS).

Note that RDSs were predicted in BECs[53] and in optical media exhibiting either Kerr[54] or non-Kerr[55] nonlinearities, while they were also observed in experiments.[56] On the other hand, RASs were only predicted to occur in non-Kerr media—for example, saturable media.[55,57] In addition, both RDS and RAS were predicted to occur in the scalar version of the nonlocal NLS.[33] Here, these structures are again found, but now as vectorial states, in the context of the multicomponent model (1)-(3). Obviously, the results of Ref. 33, together with the ones presented herein, complement this picture, as RASs (RDSs) are formed in the regime of relatively strong (weak—closer to the local Kerr nonlinearity) nonlocality.

5 | CONCLUSIONS AND DISCUSSION

In this work, we studied the formation and dynamics of vector solitons in media with a spatially nonlocal nonlinear response. The considered model, namely a two-component nonlocal NLS equation featuring a defocusing nonlinearity, finds applications in the interaction of two optical beams of different frequencies, which propagate in a doped nematic liquid crystal. We considered solutions propagating on top of a continuous-wave solution in both components, and we employed a multiscale analysis to asymptotically reduce the original model to completely integrable ones. The reduced models proved to be the well-known KP equation in the Cartesian setting, as well as its cylindrical counterpart, namely the cylindrical KP, known also as the Johnson's equation.

The version of the KP equation (KP-I or KP-II), as well as the type of the solitons (dark or antidark) that can be supported on top of the background, was found to be determined by the

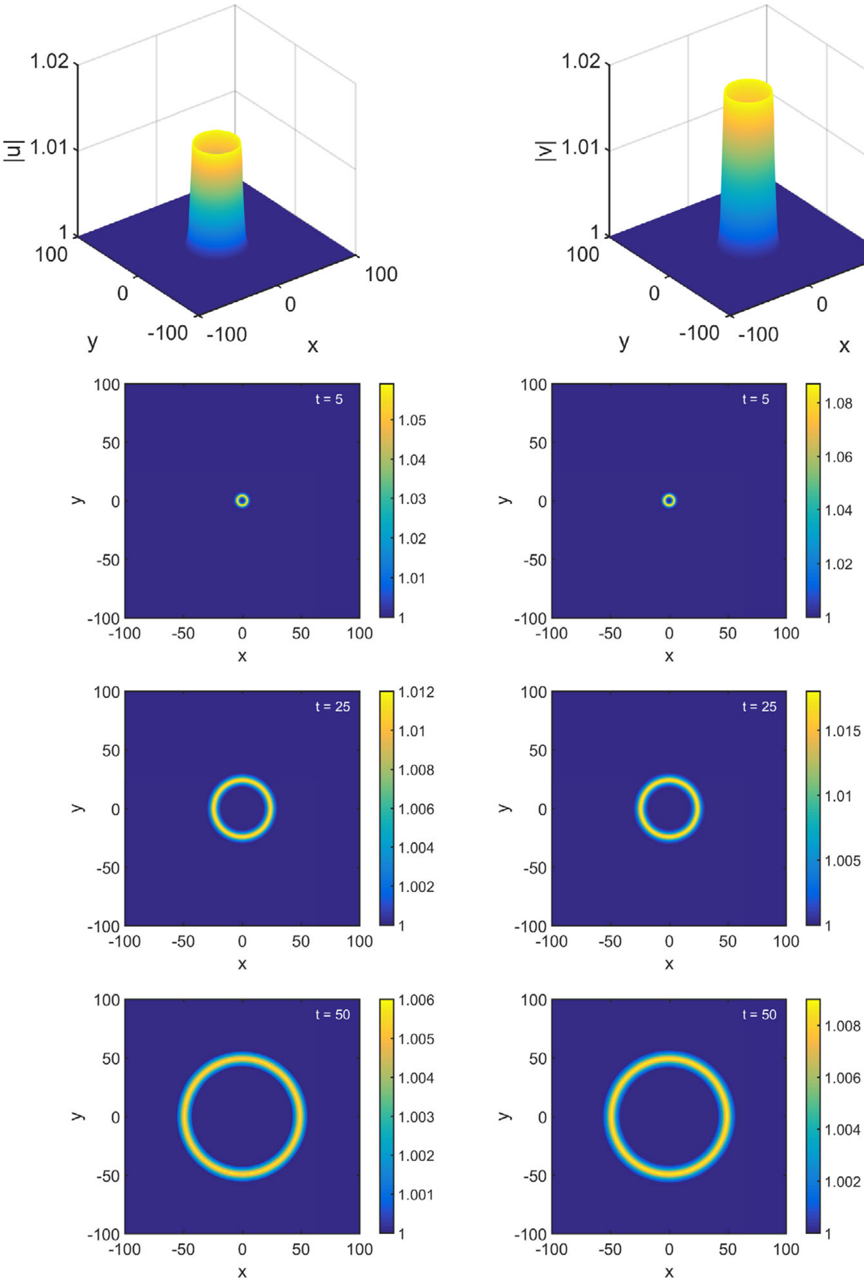

FIGURE 5 Similar to Figure 3, but now for the ring antidark soliton (RAS). In this case, parameter values are given in Equation (76), and the initial condition, at $t = 5$, is given by Equations (77)-(79), with the substitution $x \mapsto r - r_0$. Here, we again use $\varepsilon = 0.1$, and the initial ring radius is $r_0 = 4.6$

strength of the nonlocality of the original system. In particular, we found that if ν is the parameter characterizing the strength of nonlocality, then there exists a critical value ν_c depending on the parameters of the system (e.g., the dispersion and nonlinearity coefficients and the background amplitudes, such that: if $\nu > \nu_c$, then the KP equation is of KP-II type, and the solitons are

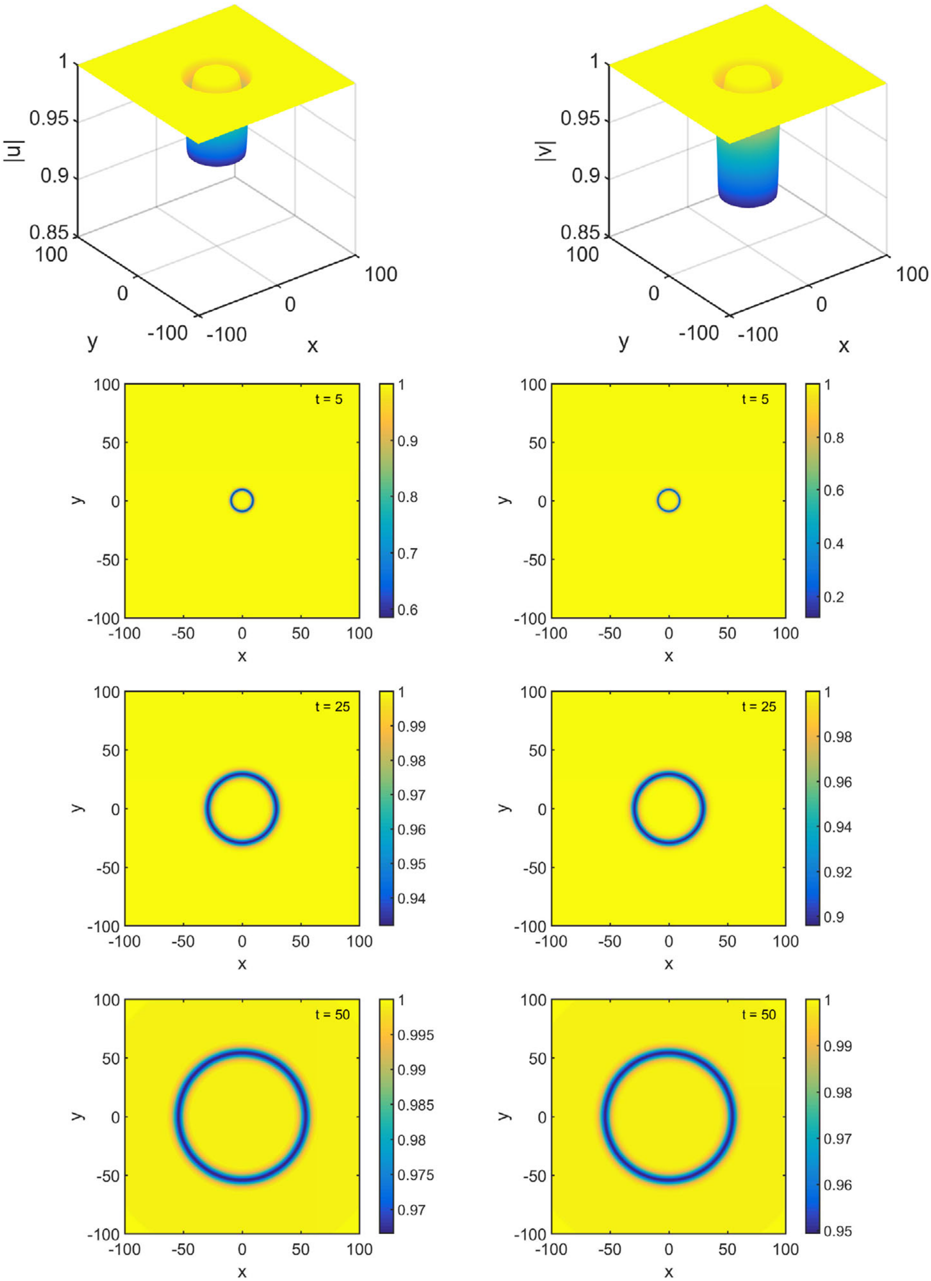

FIGURE 6 Similar to Figure 3, but now for the ring dark soliton (RDS). In this case, parameter values are given in Equation (80), and the initial condition, at $t = 5$, is given by Equations (81)-(83), with the substitution $x \mapsto r - r_0$. Here, we again use $\varepsilon = 0.1$, and the initial ring radius $r_0 = 7.37$

antidark; on the other hand, if $\nu < \nu_c$ (i.e., when nonlocality is weak and we are thus closer to the local NLS limit), then the KP equation is of KP-I type, and the solitons are dark. The change of character of the KP equation below or above the nonlocality threshold is reminiscent of a similar situation in the shallow water wave problem: if surface tension is weak, then the KP is of KP-II type, while if it is strong (in the sense that it dominates gravity), then the KP is of KP-I type. This suggests that the degree of nonlocality plays the role of an analogue of surface tension, similarly to the case of the pertinent single-component nonlocal NLS system.[34]

Our analysis reveals that the soliton amplitudes in the u- and v-components are connected to each other and thus they are governed by a single KP equation. The soliton states that we predicted to occur are: antidark and dark soliton stripes (corresponding to the stable and unstable line solitons of the KP-II and KP-I, respectively), dark lump solitons (pertinent to KP-I), as well as ring antidark and dark solitons in the cylindrical geometry. To check the validity of our predictions, we also performed direct numerical simulations (using a high-accuracy spectral method), where initial conditions were borrowed from the analytical form of the predicted KP soliton structures. We found that all types of solitons are indeed supported by the nonlocal NLS model and propagate undistorted for times (propagation distances in the context of nematic liquid crystals) up to the computation horizon. In addition, analytically predicted and numerically computed soliton velocities and decay rates (in the cylindrical case) were found to be in very good agreement. These results suggest that all the predicted solitons may be experimentally observed.

Dark soliton stripes, which correspond to the unstable line solitons of the KP-I equation, were also found to be rather robust up to the end of the simulation time. These structures are known to be prone to long-wavelength transverse perturbations in the framework of KP-I, and it is expected that this should also be the case in the context of the nonlocal NLS. A systematic investigation of the instability induced dynamics of these structures is a very interesting problem for future research. In any case, we surmise (based on the analysis and findings of Refs. 23, 24, 44) that weak dark stripe solitons will decay into lumps, which are the stable 2D soliton solutions of the KP-I equation. We also expect that this will be the case for ring dark solitons. In this case, it would be interesting to see if the onset of the transverse instability would give rise to a "lump necklace," which would follow the dynamics of the (now destroyed) ring soliton (similarly to the case of ring dark solitons that give rise to "vortex necklaces" in Bose-Einstein condensates[53]).

Our analysis and results pave the way for other interesting future research themes. For instance, it would be interesting to investigate if other, quasi one-dimensional states having, for example, the form of dark-bright soliton stripes or rings, or purely 2D structures, such as vortex-bright solitons[58] can be supported in multi-component nonlocal media. In addition, it is worth investigating the existence, stability, regularity, and radial symmetry of energy minimizing soliton solutions in our vectorial system, in the lines of the analysis performed for the scalar system.[59] Such investigations are currently in progress, and relevant results will be reported elsewhere.

ORCID

Theodoros P. Horikis https://orcid.org/0000-0003-0731-6107
Dimitrios J. Frantzeskakis https://orcid.org/0000-0002-5905-8974
Barbara Prinari https://orcid.org/0000-0001-8809-2656
Gino Biondini https://orcid.org/0000-0003-3835-1343

REFERENCES

1. Jeffrey A, Kawahara T, *Asymptotic Methods in Nonlinear Wave Theory*. London: Pitman; 1982.
2. Ablowitz MJ, Clarkson PA, *Solitons, Nonlinear Evolution Equations and Inverse Scattering*. Cambridge: Cambridge University Press; 1991.
3. Zakharov VE, Kuznetsov EA, Multi-scale expansions in the theory of systems integrable by the inverse scattering transform. *Physica D.* 1986;18:455-463.
4. Tsuzuki T, Nonlinear waves in the Pitaevskii-Gross equation. *J Low Temp Phys.* 1971;4:441-457.

5. Horikis TP, Frantzeskakis DJ, On the NLS to KdV connection. *Rom J Phys.* 2014;59:195-203.
6. Kivshar YS, Luther-Davies B, Dark optical solitons: physics and applications. *Phys Rep.* 1998;298:81-197.
7. Frantzeskakis DJ, Dark solitons in Bose-Einstein condensates: from theory to experiments. *J Phys A.* 2010;43:213001.
8. Kevrekidis PG, Frantzeskakis DJ, Carretero-González R, *The Defocusing Nonlinear Schrödinger Equation: From Dark Solitons to Vortices and Vortex Rings*. Philadelphia, PA: SIAM; 2015.
9. Litvak AG, Mironov VA, Fraiman GM, Yunakovskii AD, Thermal self-effect of wave beams in a plasma with a nonlocal nonlinearity. *Sov J Plasma Phys.* 1975;1:60-71.
10. Suter D, Blasberg T, Stabilization of transverse solitary waves by a nonlocal response of the nonlinear medium. *Phys Rev A.* 1993;48:4583-4587.
11. Rotschild C, Carmon T, Cohen O, Manela O, Segev M, Solitons in nonlinear media with an infinite range of nonlocality: first observation of coherent elliptic solitons and of vortex-ring solitons. *Phys Rev Lett.* 2005;95:213904.
12. Conti C, Peccianti M, Assanto G, Route to nonlocality and observation of accessible solitons. *Phys Rev Lett.* 2003;91:073901.
13. Pedri P, Santos L, Two-dimensional bright solitons in dipolar Bose-Einstein condensates. *Phys Rev Lett.* 2005;95:200404.
14. Urena-López LA, Brief review on scalar field dark matter models. *Front Astron Space Sci.* 2019;6:47.
15. Turitsyn SK, Spatial dispersion of nonlinearity and stability of many dimensional solitons. *Theor Math Phys.* 1985;64:797-801.
16. Krolikowski W, Bang O, Nikolov NI, Neshev D, Wyller J, Rasmussen JJ, Edmundson D, Modulational instability, solitons and beam propagation in spatially nonlocal nonlinear media. *J Opt B: Quantum Semiclass Opt.* 2004;6:S288-S294.
17. Mihalache D, Mazilu D, Lederer F, Malomed BA, Kartashov YV, Crasovan L-C, Torner L, Three-dimensional spatiotemporal optical solitons in nonlocal nonlinear media. *Phys Rev E.* 2006;73:025601(R).
18. Mihalache D, Multidimensional solitons and vortices in nonlocal nonlinear optical media. *Rom Rep Phys.* 2007;59:515-522.
19. Dreischuh A, Neshev DN, Petersen DE, Bang O, Krolikowski W, Observation of attraction between dark solitons. *Phys Rev Lett.* 2006;96:043901.
20. Kartashov YV, Torner L, Gray spatial solitons in nonlocal nonlinear media. *Opt Lett.* 2007;32:946-948.
21. Piccardi A, Alberucci A, Tabiryan N, Assanto G, Dark nematicons. *Opt Lett.* 2011;36:1356-1358.
22. Horikis TP, Small-amplitude defocusing nematicons. *J Phys A.* 2015;48:02FT01.
23. Kuznetsov EA, Turitsyn SK, Instability and collapse of solitons in media with a defocusing nonlinearity. *J Exp Theor Phys.* 1988;67:1583-1588.
24. Pelinovsky DE, Stepanyants YA, Kivshar YS, Self-focusing of plane dark solitons in nonlinear defocusing media. *Phys Rev E.* 1995;51:5016-5026.
25. Kivshar YS, Pelinovsky DE, Self-focusing and transverse instabilities of solitary waves. *Phys Rep.* 2000;331:117-195.
26. Armaroli A, Trillo S, Suppression of transverse instabilities of dark solitons and their dispersive shock waves. *Phys Rev A.* 2009;80:053803.
27. Ablowitz MJ, *Nonlinear Dispersive Waves: Asymptotic Analysis and Solitons*. Cambridge: Cambridge University Press; 2011.
28. Johnson RS, Water waves and Korteweg-de Vries equations. *J Fluid Mech.* 1980;97:701-719.
29. Infeld E, Rowlands G, *Nonlinear Waves, Solitons and Chaos*. Cambridge: Cambridge University Press; 1990.
30. Johnson RS, *A Modern Introduction to the Mathematical Theory of Water Waves*. Cambridge: Cambridge University Press; 1997.
31. Karpman VI, *Non-Linear Waves in Dispersive Media*. Amsterdam: Elsevier Science & Technology; 1974.
32. Horikis TP, Frantzeskakis DJ, Asymptotic reductions and solitons of nonlocal nonlinear Schrödinger equations. *J Phys A.* 2016;49:205202.
33. Horikis TP, Frantzeskakis DJ, Ring dark and antidark solitons in nonlocal media. *Opt Lett.* 2016;41:583-586.
34. Horikis TP, Frantzeskakis DJ, Light meets water in nonlocal media: surface tension in optics. *Phys Rev Lett.* 2017;118:243903.

35. Kevrekidis PG, Frantzeskakis DJ, Solitons in coupled nonlinear Schrödinger models: a survey of recent developments. *Rev Phys.* 2016;1:140-153.
36. Assanto G, *Nematicons: Spatial Optical Solitons in Nematic Liquid Crystals*. Hoboken, NJ: Wiley-Blackwell; 2012.
37. Assanto G, Minzoni AA, Smyth NF, Light self-localization in nematic liquid crystals: modelling solitons in nonlocal reorientational media. *J Nonlinear Opt Phys Mater.* 2009;18:657-691.
38. Alberucci A, Peccianti M, Assanto G, Dyadyusha A, Kaczmarek M, Two-color vector solitons in nonlocal media. *Phys Rev Lett.* 2006;97:153903.
39. Skuse BD, Smyth NF, Interaction of two-color solitary waves in a liquid crystal in the nonlocal regime. *Phys Rev A.* 2009;79:063806.
40. Horikis TP, Modulation instability and solitons in two-color nematic crystals. *Phys Lett A.* 2016;380:3473-3479.
41. Ablowitz MJ, Segur H, *Solitons and the Inverse Scattering Transform*. Philadelphia, PA: SIAM; 1981.
42. Infeld E, Senatorski A, Skorupski AA, Decay of Kadomtsev-Petviashvili solitons. *Phys Rev Lett.* 1994;72:1345-1347.
43. Kassam A, Trefethen LN, Fourth-order time stepping for stiff PDEs. *SIAM J Sci Comput.* 2005;26:1214-1233.
44. Mironov VA, Smirnov AI, Smirnov LA, Dynamics of vortex structure formation during the evolution of modulation instability of dark solitons. *J Exp Theor Phys.* 2011;112:46-59.
45. Wang XP, Ablowitz MJ, Segur H, Wave collapse and instability of solitary waves of a generalized Kadomtsev-Petviashvili equation. *Physica D.* 1994;78:241-265.
46. Liu Y, Wei J, Nondegeneracy, morse index and orbital stability of the KP-I lump solution. *Arch Rational Mech Anal.* 2019;234:1335-1389.
47. Oevel W, Steeb W-H, Painlevé analysis for a time-dependent Kadomtsev-Petviashvili equation. *Phys Lett A.* 1984;103:239-242.
48. Hirota R, Exact solutions to the equation describing "cylindrical solitons". *Phys Lett A.* 1979;71:393-394.
49. Santini PM, Asymptotic behaviour (in t) of solutions of the cylindrical KdV equation. - ii. *Nuovo Cimento.* 1980;57A:387-396.
50. Maxon S, Viecelli J, Cylindrical solitons. *Phys Fluids.* 1974;17:1614-1616.
51. Johnson RS, A note on an asymptotic solution of the cylindrical Korteweg-de Vries equation. *Wave Motion.* 1999;30:1-16.
52. Ko K, Kuehl HH, Cylindrical and spherical Korteweg-deVries solitary waves. *Phys Fluids.* 1979;22:1343-1348.
53. Theocharis G, Frantzeskakis DJ, Kevrekidis PG, Malomed BA, Kivshar YS, Ring dark solitons and nortex necklaces in Bose-Einstein condensates. *Phys Rev Lett.* 2003;90:120403.
54. Kivshar YS, Yang X, Ring dark solitons. *Phys Rev E.* 1994;50:R40-R43.
55. Frantzeskakis DJ, Malomed BA, Multiscale expansions for a generalized cylindrical nonlinear Schrödinger equation. *Phys Lett A.* 1999;264:179-185.
56. Dreischuh A, Neshev D, Paulus GG, Grasbon F, Walther H, Ring dark solitary waves: experiment versus theory. *Phys Rev E.* 2002;66:066611.
57. Nistazakis HE, Frantzeskakis DJ, Malomed BA, Kevrekidis PG, Head-on collisions of ring dark solitons. *Phys Lett A.* 2001;285:157-164.
58. Law KJH, Kevrekidis PG, Tuckerman LS, Stable vortex-bright-soliton structures in two-component Bose-Einstein condensates. *Phys Rev Lett.* 2010;105:160405.
59. Panayotaros P, Marchant TR, Solitary waves in nematic liquid crystals. *Physica D.* 2014;268:106-117.

How to cite this article: Koutsokostas GN, Horikis TP, Frantzeskakis DJ, Prinari B, Biondini G. Multiscale expansions and vector solitons of a two-dimensional nonlocal nonlinear Schrödinger system. *Stud Appl Math*. 2020;145:739–764. https://doi.org/10.1111/sapm.12334